Atmospheric Environment 222 (2020) 117132

Contents lists available at ScienceDirect

Atmospheric Environment

journal homepage: http://www.elsevier.com/locate/atmosenv

High-throughput, semi-automated dithiothreitol (DTT) assays for oxidative potential of fine particulate matter

Kathleen E. Berg [a], Kaylee M. Clark [a], Xiaoying Li [b], Ellison M. Carter [b], John Volckens [c,d], Charles S. Henry [a,e,*]

[a] Department of Chemistry, Colorado State University, Fort Collins, CO, 80523, USA
[b] Department of Civil & Environmental Engineering, Colorado State University, Fort Collins, CO, 80523, USA
[c] Department of Mechanical Engineering, Colorado State University, Fort Collins, CO, 80523, USA
[d] Department of Environmental & Radiological Health Sciences, Colorado State University, Fort Collins, CO, 80523, USA
[e] Department of Chemical & Biological Engineering, Colorado State University, Fort Collins, CO, 80523, USA

HIGHLIGHTS

- An automated DTT assay that uses standard HPLC equipment is presented.
- Throughputs are increased by 83% relative to manual methods.
- Detection is achieved using either electrochemical or absorbance-based methods.

GRAPHICAL ABSTRACT

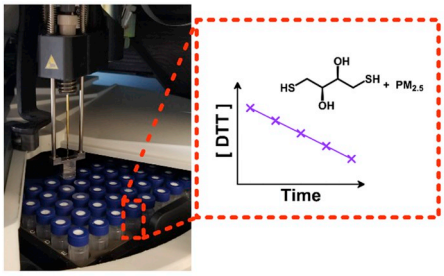

ARTICLE INFO

Keywords:
Oxidative potential
Dithiothreitol
Automated
Electrochemical
UV/vis absorbance

ABSTRACT

Fine particulate matter ($PM_{2.5}$) air pollution exposure is a leading risk factor for adverse health outcomes, including cardiovascular and respiratory morbidity, and premature mortality. Quantification of $PM_{2.5}$ oxidative potential (i.e., the ability of PM to promote oxidative reactions in solution) is a relatively new paradigm for exploring health risks associated with the various chemical compositions of ambient $PM_{2.5}$. $PM_{2.5}$ oxidative potential is commonly measured with the dithiothreitol (DTT) assay, where the DTT loss rate is measured when mixed with a $PM_{2.5}$ sample extract. However, the DTT assay is time consuming and laborious, with only a few reported automation attempts. We introduce and evaluate a semi-automated DTT assay using a traditional HPLC combined with either UV/vis absorbance or electrochemical detection that has comparable accuracy and sensitivity to manual approaches. Commercial and custom-made electrochemical detectors are also compared before measuring ambient $PM_{2.5}$ filter samples. The optimized, semi-automated assay can process six samples per hour (an 83% time savings compared to manual analysis). Cost becomes significant for large-scale studies and was also considered; electrochemical detection saved 40% on consumables cost compared to UV/vis detection. The presented liquid-handling automation can be applied to a variety of autosamplers in other laboratories for DTT assay semi-automation.

* Corresponding author. Department of Chemistry, Colorado State University, Fort Collins, CO, 80523, USA.
E-mail address: chuck.henry@colostate.edu (C.S. Henry).

https://doi.org/10.1016/j.atmosenv.2019.117132
Received 19 June 2019; Received in revised form 25 October 2019; Accepted 9 November 2019
Available online 23 November 2019
1352-2310/

1. Introduction

Human exposure to fine particulate matter ($PM_{2.5}$, particles with aerodynamic diameter less than 2.5 μm) is a leading contributor to the global burden of disease with a well-established link to several million premature deaths annually, as well as millions of cardiovascular- and respiratory-related hospitalizations (Cohen et al., 2017; Morakinyo et al., 2016; Hoek et al., 2013; Gakidou et al., 2017). In 2015, $PM_{2.5}$ exposure was estimated to contribute to 4.2 million premature deaths (7.6% of total global mortality). A recent study estimated that achieving the World Health Organization's air quality guideline of 10 $\mu g/m^3$ (as an annual average outdoor $PM_{2.5}$ concentration) would result in life expectancy increases of 0.6 years, the same magnitude as eliminating *both* breast and lung cancer worldwide (Apte et al., 2018). Current air quality regulations focus on limiting the mass concentration of $PM_{2.5}$ in outdoor air; however, recent research suggests that PM mass concentration is likely an imperfect predictor of risk for health effects because the composition (and potential toxicology) of PM can vary substantially even though mass concentration may remain constant (Borm et al., 2007; Cho et al., 2005; Crobeddu et al., 2017; Forman and Finch, 2018; Ntziachristos et al., 2007). A leading hypothesis for $PM_{2.5}$ toxicity is that $PM_{2.5}$ generates reactive oxygen species (ROS), which leads to oxidative stress and systemic inflammation (Alfadda and Sallam, 2012; Anderson et al., 2012; De Vizcaya-Ruiz et al., 2006; Campbell et al., 2005; Bates et al., 2015). Thus, the oxidative potential (ability to oxidize target molecules) of PM has been proposed as a complementary measure to $PM_{2.5}$ mass concentration (Borm et al., 2007; Brook et al., 2010; Janssen et al., 2014).

A widely used chemical assay to estimate PM oxidative potential is the dithiothreitol (DTT) assay (Verma et al., 2014; Fang et al., 2015a; Visentin et al., 2016; Xiong et al., 2017; Bates et al., 2018, 2019), which has been positively correlated with biological markers that correspond to oxidative stress and inflammation biomarkers (Crobeddu et al., 2017; Li et al., 2003). To perform the assay, DTT is mixed with the extracted $PM_{2.5}$ sample, and the remaining DTT is quantified over time (the rate of DTT loss is related to the PM oxidative potential). Despite the widespread use of the DTT assay, there is not a singular protocol practiced across all laboratories. In the original published assay (Cho et al., 2005), a known (but variable amount between 5 and 40 μg/mL) PM sample concentration was incubated with 100 μM DTT in pH 7.4 potassium phosphate buffer at 37 °C. Trichloroacetic acid was added to quench the reaction at various times between 15 and 90 min, and an aliquot was removed and mixed with ethylenediaminetetraacetic acid (EDTA) and 5, 5-dithio-bis-(2-nitrobenzoic acid) (Ellman's reagent, DTNB). DTNB reacts with DTT to form 5-mercapto-2-nitrobenzoic acid (TNB), which is quantified spectroscopically at 412 nm. Since the initial publication, subsequent studies have varied the following filter preparation and DTT assay parameters: the incubated concentration of PM (Charrier et al., 2016), the addition of a filter wetting agent (Vidrio et al., 2009), the time points at which DTT concentration is measured (Berg et al., 2019; Fang et al., 2015b), the quenching reagent (Sameenoi et al., 2012), the use of Chelex instead of EDTA (Charrier and Anastasio, 2012), and an alternative DTT detection method (Sameenoi et al., 2012). The modifications were typically made to improve the assay, but the inconsistencies among the DTT assays can cause confusion and lead to uncertainties when comparisons are made between results from different protocols.

The DTT assay, as originally published, has the major limitation of being labor and time intensive, having long turnaround time from sample collection to results, and requiring many reagents. To address these problems, there have been several reports of semi-automated assays that reduce time and reagents (Berg et al., 2019; Fang et al., 2015b; Sameenoi et al., 2012, 2013; Samake et al., 2017; Koehler et al., 2014). Samake et al. used a plate reader to automate a portion of the UV/vis detection. While this approach was an improvement, no automation of liquid handling was noted (Samake et al., 2017). Another study shortened the results turnaround time to 30 min by utilizing a microfluidic paper-based analytical device (μPAD), but this assay would be difficult to automate (Sameenoi et al., 2013). An alternative electrochemical detection method presented by Sameenoi et al. eliminates trichloroacetic acid and DTNB (and associated costs and labor), while also enabling online monitoring when coupled to a particle-into-liquid sampler (PILS) (Sameenoi et al., 2012; Koehler et al., 2014). Another online DTT assay that uses a mist chamber and automated syringe pump has also been developed (Puthussery et al., 2018). We recently reported a higher analysis rate to five samples per hour with one person (as compared to one sample per hour with two persons (Fang et al., 2015b)) using electrochemical detection (Berg et al., 2019), but our approach did not yet automate liquid handling. The only report we found thus far using liquid handling automation is by Fang et al., where programmable syringe pumps were used to develop the most automated DTT assay reported to date (Fang et al., 2015b). The system can analyze approximately one sample per hour, be left unattended for 24 h, and be monitored remotely. To our knowledge, while there are many advantages to this assay relative to the fully manual system, the sample processing rate is still relatively slow.

The objective of the work herein was to develop an alternative approach to a semi-automated DTT assay with the following characteristics: higher sample throughput than previous semi-automated systems, modifications from the original assay, and accessible to other laboratories with similar equipment. The system uses a high-performance liquid chromatography (HPLC) pump and autosampler programmed to mix reagents and inject aliquots. We demonstrate use of the system with $PM_{2.5}$ filter samples using two detection options: UV/vis absorbance (already integrated into the HPLC) and electrochemical (custom-made or commercially available flow cell integrated into the HPLC). The developed method here has comparable accuracy and precision as the previously published DTT assays. Both detection options have sampling rates of six samples per hour, equivalent to an 83% time savings compared to the existing semi-automated systems. The non-reusable products (i.e. consumables) associated with the electrochemical detection presents a 40% cost savings relative to the UV/vis detection. The liquid automation concepts used to develop this technique can be applied towards other similar HPLCs and autosamplers.

2. Materials and methods

All chemicals used were reagent grade and used as received with solution preparation in 18.2 MΩ cm water (MilliPore Milli-Q system, Billerica, MA, USA). DTT was purchased from Acros Organics (NJ, USA). Copper (II) sulfate ($CuSO_4$), DTNB, Chelex® 100 resin, potassium phosphate monobasic, and potassium phosphate dibasic were purchased from Sigma-Aldrich (MO, USA). An Ultimate 3000 HPLC (Thermo Fisher Scientific, MA, USA) was used with a pH 7.4 phosphate buffer eluent at 1 mL/min for the UV/vis detection and electrochemical detection with the custom thermoplastic electrode (TPE) flow cell. The commercial electrochemical flow cell (FLWCL, DropSens, Spain) was run with a commercial 3-electrode set up (DropSens 410 SPE, DropSens, Spain) with a pH 7.4 phosphate buffer eluent at 0.085 mL/min. Details related to the custom TPE electrochemical flow cell construction are provided in the Supporting Information. All electrochemical experiments were operated using a PalmSens4 potentiostat and peak height (as customary with electrochemical wall jet flow cells (Albery and Brett, 1983; Yamada and Matsuda, 1973)) was analyzed using PSTrace software (Palmsens, Houten, Netherlands).

2.1. Filter sampling

Ambient $PM_{2.5}$ samples were collected in two neighboring (~2 km) villages in Yu County (112.55°–113.49° E, 37.57°–38.31° N) of Yangquan City, Shanxi Province in China. Yu County is in the east of Shanxi Province and southwest of Beijing, approximately 400 km away. The

two villages where sampling took place are located approximately 9–10 km from the primary urban center of Yu County. One four-channel sampler (Gas village: TH-16 A, Tianhong, China; Coal village: RT-AP4, Ruite, China) was set up to collect 24-h ambient $PM_{2.5}$ samples in the center of each village. The flow rate of the sampler was 16.7 L/min. Two 47 mm PTFE and quartz filters were collected at the same time. Four sets of field blanks were collected at both sites. In total, 36 sets of PTFE and quartz filters were collected from January 1–24, 2018. All filter samples were transported to the field laboratory and immediately stored in a −20 °C freezer. Following completion of the field sampling campaign, all samples were transported by plane to Colorado State University, where they were stored in a −20 °C freezer prior to mass measurement and oxidative potential analyses. The PTFE filters (Zefluor, Pall Life Sciences) were conditioned for 24-h (21–22 °C, 30–34% humidity) and weighed in triplicate on a microbalance (Mettler Toledo XS3DU) with 1-μg resolution before and after sample collection. The average of the three readings was taken as each filter weight, unless two weights differed by more than 5 μg, in which case the filters were weighed more times until there were three weights within 5 μg. Filter gross masses were blank-corrected using the mean value of blank filters (8 ± 8 μg), and $PM_{2.5}$ concentrations were calculated by dividing blank-corrected values by the sampled air volume.

Air sampling filters were collected from March 3 through April 30, 2015 as part of a Honduras cookstove study as previously reported (Berg et al., 2019; Rajkumar et al., 2018). One blank filter was collected every two weeks. $PM_{2.5}$ was sampled onto 37-mm PTFE-coated glass fiber filters (Fiberfilm™ T60A20, Pall Corporation, KY, USA) using Triplex Cyclones (BGI, Mesa Labs, Butler NJ, USA) and AirChek XR5000 pumps (SKC Inc., Eighty Four, PA, USA) operating at 1.5 L/min for 24 h. The filters were equilibrated for at least 24 h and then pre-weighed to the nearest microgram at Colorado State University (CSU) using a microbalance (Mettler-Toledo microbalance model MX5, Columbus, OH, USA). After collection of the $PM_{2.5}$ sample, filters were stored at −22 °C and then transported to CSU, equilibrated, and post-weighed. The filters were then stored in a −80 °C freezer until tested. Filters were collected near the participant's breathing zone or 76–127 cm from the stovetop in the participants' kitchens.

2.2. Automated DTT assay system

0.1 M potassium phosphate, pH 7.4 buffer was Chelex®-treated for at least one week and the Chelex® was decanted and filtered prior to use. Air sampling filters were handled with ceramic scissors and plastic forceps to avoid metal contamination. The filters were cut and weighed to achieve a target concentration of 10 μg PM per mL buffer while using between 100 and 1500 μL total buffer volume (different volumes of buffer were added as determined by the weight of the filter piece). Before buffer addition, the filters were wetted with 15 μL of 50:50 TFE: water (v:v) in a 1.5 mL centrifuge tube. The calculated amount of buffer was added to achieve 10 μg PM/mL buffer, and the samples were sonicated at 37 °C for 30 min. 90 μL was removed from the centrifuge tubes into HPLC vials (300 μL polypropylene plastic, Waters, MA, USA). 10 μL of 1 mM DTT (100 μM final concentration) was added to each vial, including a blank buffer for each sample set, and mixed with either a multi-channel pipette (Integra Voyager, Integra Biosciences Corp, NH, USA) or by the HPLC. For UV/vis absorbance detection, two vials of each extracted PM were prepared (initial and 35 min). After a known reaction time, 10 μL of 3 mM DTNB in buffer was injected and mixed into the DTT vial. Three separate 10 μL aliquots were injected into the HPLC UV/vis detector at 412 nm for a total of six measurements per sample. Peak area was used for DTT calibration and subsequent quantification. For electrochemical detection, a 10 μL aliquot was injected into the electrochemical flow cell; this injection was repeated five times (n = 6 total) unless otherwise stated. The potentiostat was held at +0.3 V vs Ag/AgCl, and current was measured. Current peak height (Ip, $\mu A/cm^2$) was used for DTT calibration and subsequent quantification. The instrument signal, either absorbance or current, from the various time points was converted to DTT concentration (in nmol) using the calibration curve values. The DTT rate, nmol per min, was calculated using Microsoft Excel's linear best fit slope and uncertainty (LINEST function). The blank rate (calculated the same way via the best fit slope) is subtracted from the DTT rate. The DTT rate uncertainty is calculated from propagating the DTT rate and blank rate uncertainties, as previously reported (Charrier et al., 2015). The DTT rate, nmol per min, is divided by the PM solution concentration (10 μg/mL in all cases here as previously discussed) and the total volume of air sampled (2.16 m^3), which leads to units of nmol min^{-1} μg^{-1} m^{-3}. The HPLC program used can be found in the Supporting Information.

3. Results and discussion

We sought to provide a higher throughput alternative approach to conducting the DTT assay by programming an HPLC to perform the liquid handling steps after $PM_{2.5}$ collected on filters are extracted in TFE and buffer. The automation was initially performed using an HPLC pump, autosampler, and UV/vis detector. Example peaks and the resulting DTT calibration curve are shown in Fig. 1. DTT detection linearity, sensitivity, and precision are evident from the calibration curve, and the coefficient of determination (R^2) is 0.991. Relative standard deviation was ≤5% at each DTT concentration. For the DTT assay to measure oxidative potential, the HPLC was programmed to inject and mix DTT into a vial containing sample, followed by DTNB, and then finally injecting a sample aliquot for detection. Two vials were used for each extracted filter sample for two separate time points (0 and 35 min) for an end-point assay. The programmed mixing consists of withdrawing the final solution volume from the vial and reinjecting it into the same vial using the HPLC's integrated syringe. The DTNB was then injected and mixed into each vial. Automating DTT and DTNB injection and mixing into the samples provided a throughput rate of three samples per hour. When a multi-channel pipette was used to inject and mix the DTT with the same volumes, the sample throughput rate doubled to six samples per hour with three DTT measurements at each of the two time points. If the multi-channel pipette was used, the DTNB was still added and mixed using the HPLC. The multi-channel pipette needs slightly more manual labor (less than a minute per sample), but it doubles the sample throughput rate.

The system's accuracy was tested with Cu(II) as a positive control to compare DTT oxidation rate to the manual DTT assay (Fig. 2). The

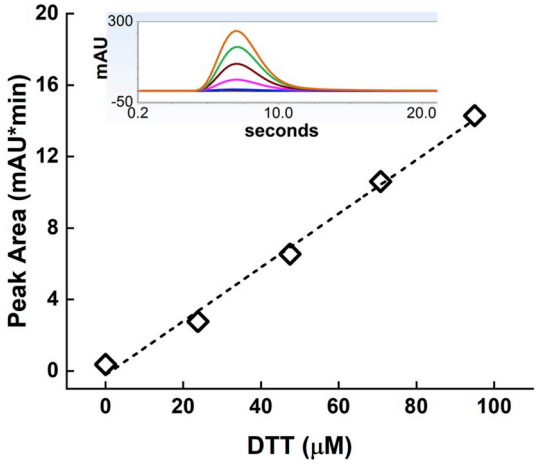

Fig. 1. Example HPLC UV/vis detection peaks (inset) and corresponding calibration curve. The dashed line is the linear regression with Peak Area=(0.150 ± 0.007)[DTT]-(0.2 ± 0.4), R^2 of 0.991. Standard deviation error bars (all ≤5% relative standard deviation) are not visible from n = 5 replicate measurements conducted at each DTT concentration.

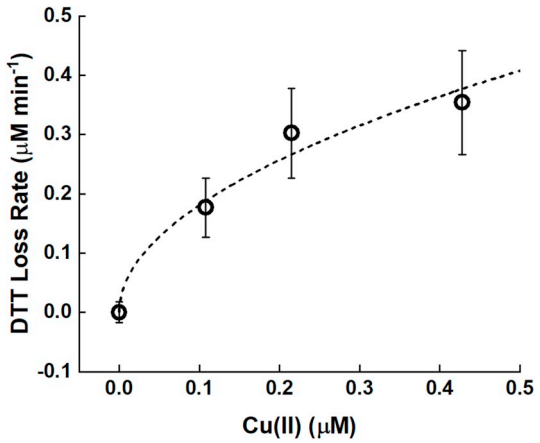

Fig. 2. DTT reaction rate at four Cu(II) concentrations. The dashed line is the best fit line, where DTT rate = $0.58[Cu]^{0.5}$. Error bars represent the standard deviation from the linear DTT rates at each Cu concentration (n = 6).

published blank-subtracted DTT reaction rate (μM min^{-1}) is $1.06[Cu]^{0.442}$ (Charrier and Anastasio, 2012). Our measured blank-subtracted DTT reaction rate (μM min^{-1}) was $0.58[Cu]^{(0.5\pm0.1)}$, where the uncertainty is the 95% confidence interval of the fit from the four Cu(II) concentrations. The error bars represent the standard deviation from six measurements at each Cu(II) concentration. Our measured reaction rate constant of 0.58 is lower than the published value of 1.06, likely because the DTT loss rate was performed at room temperature whereas the literature value is measured at 37 °C and given the dependence of the reaction rate constant on solution conditions (e.g. temperature, pH, ionic strength). The literature partial order, 0.442, does fall within the 95% confidence interval of our measured partial order of 0.5 ± 0.1, and demonstrates that the DTT in this study is likely reacting as it has in previous studies.

The DTT assay with electrochemical detection requires fewer reagents while providing comparable sensitivity to UV/vis detection. Instead of injecting and mixing the DTNB before removing an aliquot of sample solution for analysis, an aliquot was taken at various times after the DTT reaction began. The aliquot was injected into an electrochemical flow cell instead of the HPLC's UV/vis detector. Electrochemical detection with a commercial flow cell was tested. The commercial flow cell is advantageous to laboratories without electrochemical fabrication equipment. However, the maximum flow rate of the commercial flow cell is 0.085 mL/min. The injections are synchronized with the HPLC pump to ensure reproducibility, and the lower flow rate caused a delay in the injection rate to ensure the injection was synchronized with the pump. The injection time delay resulted in a sampling rate of three samples per hour when using the commercial flow cell. Example DTT injection peaks and calibration curve are shown in Fig. 3. Filter samples were not tested with the commercial flow cell because of the lower flow rate. Numerous commercial electrochemical flow cells exist and can be tested at a higher flow rate to achieve a higher sampling rate.

To achieve higher flow rates (and thus higher sampling rates) in an electrochemical flow cell, we designed and fabricated a custom electrochemical flow cell (Klunder et al., 2017) using a composite carbon electrode (details in the Supporting Information). The flow cell costs less than $1, is reusable by polishing the electrode surface until the 6-mm thick electrode material is gone, and has a maximum flow rate >1 mL/min. The higher flow rate allowed for a sampling rate of about double than the commercial electrochemical flow cell. Example DTT injection peaks and calibration curves are shown in Fig. 3. For the electrochemical DTT assay, we opted not use a quenching reagent to save time and consumables. Measuring only two time points here would not give uncertainty in the measurements because replicates cannot be done at the same reaction time, as with the UV/vis assay. The linear least squares regression uncertainty with the lab blank uncertainty propagated (as a real sample would be numerically treated) was calculated with an increasing number of time points (Fig. 4) from five filter samples, collected as described elsewhere (Rajkumar et al., 2018). There are significant differences ($p < 0.05$, ANOVA one-way test performed with Microsoft Excel) in the filter sample rate uncertainties based on the number of injections, from three to six. The F-critical value was 5.32 with F values of 47.31 (three vs four injections), 50.71 (four vs five), and 7.60 (five vs six). The blank was not included in the calculations. There were not significant differences in the uncertainties between six and seven injections ($p > 0.05$, F value of 3.31). Therefore, six time points (injections) were used in the electrochemical detection study (n = 6). The impact of decreasing uncertainty can also be seen in Fig. 4. The blank-subtracted rates of the corresponding filters are also shown, where the black dotted line is the blank rate ± uncertainty. All of the rates are within the blank rate uncertainty until over five injection time points.

After measuring accuracy, precision, and sensitivity of the semi-automated system with UV/vis or electrochemical detection, real filter samples were analyzed from two different locations (Fig. 5) that vary with respect to aerosol abundance and composition. The semi-automated system successfully measured the oxidative potential of 59

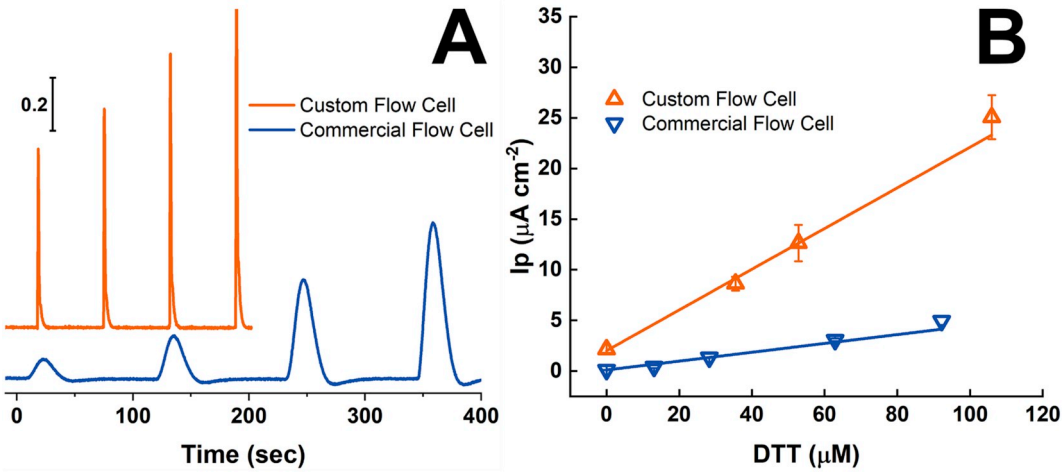

Fig. 3. Examples of electrochemical DTT detection injection peaks (A, scale bar is 0.2 μA) and calibration curves (B) comparing the custom and commercial DropSens electrochemical flow cells. The linear regression for the custom flow cell calibration curve is (0.218 ± 0.009)[DTT]+(1.5 ± 0.6), R^2 of 0.973, and the commercial flow cell is (0.053 ± 0.003)[DTT]-(0.1 ± 0.1), R^2 of 0.993. Error bars represent one standard deviation about the mean (n = 4).

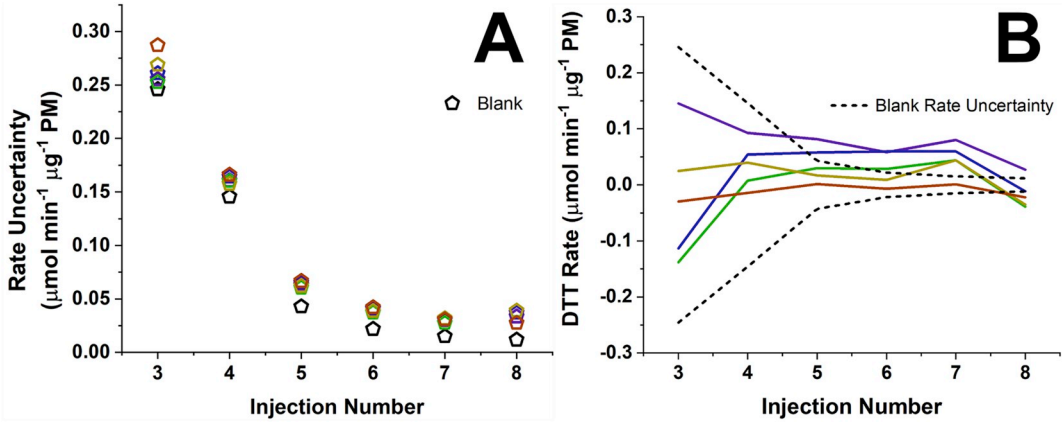

Fig. 4. The DTT rate uncertainty, determined from repeated analysis of samples extracted from multiple different filter-based samples, as a function of the number of injections (A). The blank error was propagated. The corresponding filters' blank-subtracted rates (B). The two dashed black lines are the blank rate ± uncertainty.

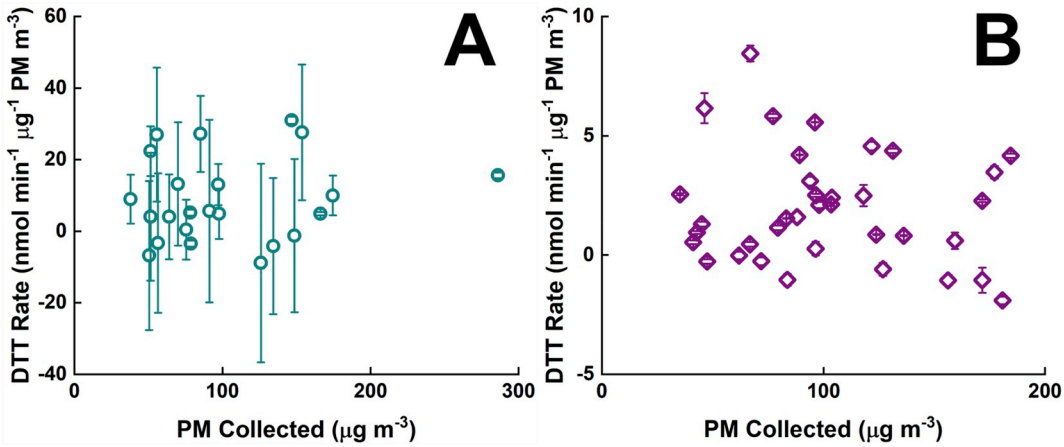

Fig. 5. DTT rates of $PM_{2.5}$ filter samples from different sources tested with electrochemical detection (A, dark cyan circle, source: Honduras) and the automated UV/vis detection (B, purple diamond, source: China). Error bars represent linear regression uncertainty from n = 6. (For interpretation of the references to colour in this figure legend, the reader is referred to the Web version of this article.)

ambient $PM_{2.5}$ filter samples in under 10 h (each unique sample was analyzed six times). The varied standard deviations between ambient $PM_{2.5}$ samples collected in Honduras have been seen before with these same samples using either detection motif and therefore are likely not a result of the detection method used, also as previously discussed (Berg et al., 2019). The differences between the standard deviations between the two collection sites can likely be attributed to the $PM_{2.5}$ components in each of the samples and each of their corresponding filter extraction efficiencies, DTT oxidation rates, and uncertainty (Charrier and Anastasio, 2012; Bein and Wexler, 2015).

Both the UV/vis and electrochemical detection (with the custom flow cell) allowed for an analysis rate of six samples per hour, and the manual labor was only associated with the sample preparation. The sensitivities (instrument response per unit concentration of DTT, calculated from the DTT calibration curves) of the UV/vis and electrochemical detection are 0.150 mAU*min/μM DTT and 0.218 Ip/μM DTT, respectively. Although these reported sensitivities are different, they are comparable and more than sufficient for the DTT assay. The current consumables cost per sample (as calculated upon publication) of the UV/vis detection is $2.50, but the electrochemical detection is cheaper at $1.50 per sample (Table 1), equivalent to the electrochemical detection providing a 40% cost savings per 100 filters analyzed. The cost difference is a result of the extra reagents and vials required for the UV/vis detection. The electrochemical detection does require a flow cell and a potentiostat. Our custom electrochemical flow cell is reusable and costs less than $1, while the commercial DropSens flow cell is currently about $1000 with reusable (up to about 30 injections) electrodes. Even though we used a Thermo Fisher Scientific HPLC here for the liquid handling, other autosamplers and flow pumps are likely suitable for DTT assay automation. Reducing cost and time associated with performing DTT assays with aerosol samples can lower barriers to incorporating oxidative potential analysis at a larger scale in exposure, environmental health, and epidemiologic studies. Doing so could provide new insight on spatial and temporal patterning in multiple PM measurements, including personal exposures. The DTT assay provides a measure of oxidative activity associated with the PM in the sample, and this may shed important light on human health impacts of particulate matter pollution, a leading environmental health risk factor worldwide.

Table 1
Comparison between semi-automated UV/vis absorbance detection and electrochemical detection with our custom electrochemical flow cell or a commercial DropSens electrochemical flow cell.

	UV/Vis	Custom	Commercial
Rate (samples per hour)	6	6	3
Consumables Cost ($ per sample)	2.50	1.50	1.60
Sensitivity (per μM DTT)	0.150 mAU min	0.218 μA cm^{-2}	0.053 μA cm^{-2}
Other Equipment Needed		Potentiostat	Potentiostat

Declaration of competing interest

The authors declare that they have no known competing financial interests or personal relationships that could have appeared to influence the work reported in this paper.

Acknowledgements

Funding for this research was provided through the National Institutes of Health (ES024719), National Institute for Occupational Safety and Health (OH010662), and the National Science Foundation (1710222).

Appendix A. Supplementary data

Supplementary data to this article can be found online at https://doi.org/10.1016/j.atmosenv.2019.117132.

References

Albery, W.J., Brett, C.M., 1983. The wall-jet ring-disc electrode: Part ii. Collection efficiency, titration curves and anodic stripping voltammetry. J. Electroanal. Chem. Interfacial Electrochem. 148 (2), 211–220.
Alfadda, A.A., Sallam, R.M., 2012. Reactive oxygen species in health and disease. BioMed Res. Int. 2012.
Anderson, J.O., Thundiyil, J.G., Stolbach, A., 2012. Clearing the air: a review of the effects of particulate matter air pollution on human health. J. Med. Toxicol. 8 (2), 166–175.
Apte, J.S., Brauer, M., Cohen, A.J., Ezzati, M., Pope, C.A., 2018. Ambient pm2.5 reduces global and regional life expectancy. Environ. Sci. Technol. Lett.
Bates, J.T., Weber, R.J., Abrams, J., Verma, V., Fang, T., Klein, M., Strickland, M.J., Sarnat, S.E., Chang, H.H., Mulholland, J.A., Tolbert, P.E., Russell, A.G., 2015. Reactive oxygen species generation linked to sources of atmospheric particulate matter and cardiorespiratory effects. Environ. Sci. Technol. 49 (22), 13605–13612.
Bates, J.T., Weber, R.J., Verma, V., Fang, T., Ivey, C., Liu, C., Sarnat, S.E., Chang, H.H., Mulholland, J.A., Russell, A., 2018. Source impact modeling of spatiotemporal trends in pm2.5 oxidative potential across the eastern United States. Atmos. Environ. 193, 158–167.
Bates, J.T., Fang, T., Verma, V., Zeng, L., Weber, R.J., Tolbert, P.E., Abrams, J.Y., Sarnat, S.E., Klein, M., Mulholland, J.A., Russell, A.G., 2019. Review of acellular assays of ambient particulate matter oxidative potential: methods and relationships with composition, sources, and health effects. Environ. Sci. Technol. 53 (8), 4003–4019.
Bein, K., Wexler, A., 2015. Compositional variance in extracted particulate matter using different filter extraction techniques. Atmos. Environ. 107, 24–34.
Berg, K.E., Turner, L.R., Benka-Coker, M.L., Rajkumar, S., Young, B.N., Peel, J.L., Clark, M.L., Volckens, J., Henry, C.S., 2019. Electrochemical dithiothreitol assay for large-scale particulate matter studies. Aerosol Sci. Technol. 1–8.
Borm, P.J.A., Kelly, F., Künzli, N., Schins, R.P.F., Donaldson, K., 2007. Oxidant generation by particulate matter: from biologically effective dose to a promising, novel metric. Occup. Environ. Med. 64 (2), 73–74.
Brook, R.D., Rajagopalan, S., Pope, C.A., Brook, J.R., Bhatnagar, A., Diez-Roux, A.V., Holguin, F., Hong, Y., Luepker, R.V., Mittleman, M.A., Peters, A., Siscovick, D., Smith, S.C., Whitsel, L., Kaufman, J.D., 2010. Particulate matter air pollution and cardiovascular disease. Update Sci. Statement Am. Heart Assoc. 121 (21), 2331–2378.
Campbell, A., Oldham, M., Becaria, A., Bondy, S., Meacher, D., Sioutas, C., Misra, C., Mendez, L., Kleinman, M., 2005. Particulate matter in polluted air may increase biomarkers of inflammation in mouse brain. Neurotoxicology (Little Rock) 26 (1), 133–140.
Charrier, J.G., Anastasio, C., 2012. On dithiothreitol (dtt) as a measure of oxidative potential for ambient particles: evidence for the importance of soluble transition metals. Atmos. Chem. Phys. 12 (5), 11317–11350.
Charrier, J., Richards-Henderson, N., Bein, K., McFall, A., Wexler, A., Anastasio, C., 2015. Oxidant production from source-oriented particulate matter–part 1: oxidative potential using the dithiothreitol (dtt) assay. Atmos. Chem. Phys. 15 (5), 2327–2340.
Charrier, J.G., McFall, A.S., Vu, K.K.T., Baroi, J., Olea, C., Hasson, A., Anastasio, C., 2016. A bias in the "mass-normalized" dtt response – an effect of non-linear concentration-response curves for copper and manganese. Atmos. Environ. 144, 325–334.
Cho, A.K., Sioutas, C., Miguel, A.H., Kumagai, Y., Schmitz, D.A., Singh, M., Eiguren-Fernandez, A., Froines, J.R., 2005. Redox activity of airborne particulate matter at different sites in the los angeles basin. Environ. Res. 99 (1), 40–47.
Cohen, A.J., Brauer, M., Burnett, R., Anderson, H.R., Frostad, J., Estep, K., Balakrishnan, K., Brunekreef, B., Dandona, L., Dandona, R., Feigin, V., Freedman, G., Hubbell, B., Jobling, A., Kan, H., Knibbs, L., Liu, Y., Martin, R., Morawska, L., Pope III, C.A., Shin, H., Straif, K., Shaddick, G., Thomas, M., van Dingenen, R., van Donkelaar, A., Vos, T., Murray, C.J.L., Forouzanfar, M.H., 2017. Estimates and 25-year trends of the global burden of disease attributable to ambient air pollution: an analysis of data from the global burden of diseases study 2015. The Lancet 389 (10082), 1907–1918.
Crobeddu, B., Aragao-Santiago, L., Bui, L.-C., Boland, S., Baeza Squiban, A., 2017. Oxidative potential of particulate matter 2.5 as predictive indicator of cellular stress. Environ. Pollut. 230, 125–133.
De Vizcaya-Ruiz, A., Gutiérrez-Castillo, M., Uribe-Ramirez, M., Cebrián, M., Mugica-Alvarez, V., Sepúlveda, J., Rosas, I., Salinas, E., Garcia-Cuéllar, C., Martínez, F., 2006. Characterization and in vitro biological effects of concentrated particulate matter from Mexico city. Atmos. Environ. 40, 583–592.
Fang, T., Verma, V., Bates, J., Abrams, J., Klein, M., Strickland, M., Sarnat, S., Chang, H., Mulholland, J., Tolbert, P., 2015a. Oxidative potential of ambient water-soluble pm 2.5 measured by dithiothreitol (dtt) and ascorbic acid (aa) assays in the southeastern United States: contrasts in sources and health associations. Atmos. Chem. Phys. Discuss. 15 (21).
Fang, T., Verma, V., Guo, H., King, L., Edgerton, E., Weber, R., 2015b. A semi-automated system for quantifying the oxidative potential of ambient particles in aqueous extracts using the dithiothreitol (dtt) assay: results from the southeastern center for air pollution and epidemiology (scape). Atmos. Meas. Tech. 8 (1), 471.
Forman, H.J., Finch, C.E., 2018. A critical review of assays for hazardous components of air pollution. Free Radic. Biol. Med. 117, 202–217.
Gakidou, E., Afshin, A., Abajobir, A.A., Abate, K.H., Abbafati, C., Abbas, K.M., Abd-Allah, F., Abdulle, A.M., Abera, S.F., Aboyans, V., 2017. Global, regional, and national comparative risk assessment of 84 behavioural, environmental and occupational, and metabolic risks or clusters of risks, 1990–2016: a systematic analysis for the global burden of disease study 2016. The Lancet 390 (10100), 1345–1422.
Hoek, G., Krishnan, R.M., Beelen, R., Peters, A., Ostro, B., Brunekreef, B., Kaufman, J.D., 2013. Long-term air pollution exposure and cardio-respiratory mortality: a review. Environ. Health 12 (1), 43.
Janssen, N.A.H., Yang, A., Strak, M., Steenhof, M., Hellack, B., Gerlofs-Nijland, M.E., Kuhlbusch, T., Kelly, F., Harrison, R., Brunekreef, B., Hoek, G., Cassee, F., 2014. Oxidative potential of particulate matter collected at sites with different source characteristics. Sci. Total Environ. 472, 572–581.
Klunder, K.J., Nilsson, Z., Sambur, J.B., Henry, C.S., 2017. Patternable solvent-processed thermoplastic graphite electrodes. J. Am. Chem. Soc. 139 (36), 12623–12631.
Koehler, K.A., Shapiro, J., Sameenoi, Y., Henry, C., Volckens, J., 2014. Laboratory evaluation of a microfluidic electrochemical sensor for aerosol oxidative load. Aerosol Sci. Technol. 48 (5), 489–497.
Li, N., Sioutas, C., Cho, A., Schmitz, D., Misra, C., Sempf, J., Wang, M., Oberley, T., Froines, J., Nel, A., 2003. Ultrafine particulate pollutants induce oxidative stress and mitochondrial damage. Environ. Health Perspect. 111 (4), 455.
Morakinyo, O.M., Mokgobu, M.I., Mukhola, M.S., Hunter, R.P., 2016. Health outcomes of exposure to biological and chemical components of inhalable and respirable particulate matter. Int. J. Environ. Res. Public Health 13 (6), 592.
Ntziachristos, L., Froines, J.R., Cho, A.K., Sioutas, C., 2007. Relationship between redox activity and chemical speciation of size-fractionated particulate matter. Part. Fibre Toxicol. 4 (1), 5.
Puthussery, J.V., Zhang, C., Verma, V., 2018. Development and field testing of an online instrument for measuring the real-time oxidative potential of ambient particulate matter based on dithiothreitol assay. Atmos. Meas. Tech. 11 (10), 5767–5780.
Rajkumar, S., Clark, M.L., Young, B.N., Benka-Coker, M.L., Bachand, A.M., Brook, R.D., Nelson, T.L., Volckens, J., Reynolds, S.J., L'Orange, C., 2018. Exposure to household air pollution from biomass-burning cookstoves and hba1c and diabetic status among honduran women. Indoor Air.
Samake, A., Uzu, G., Martins, J., Calas, A., Vince, E., Parat, S., Jaffrezo, J., 2017. The unexpected role of bioaerosols in the oxidative potential of pm. Sci. Rep. 7 (1), 10978.
Sameenoi, Y., Koehler, K., Shapiro, J., Boonsong, K., Sun, Y., Collett, J., Volckens, J., Henry, C.S., 2012. Microfluidic electrochemical sensor for on-line monitoring of aerosol oxidative activity. J. Am. Chem. Soc. 134 (25), 10562–10568.
Sameenoi, Y., Panymeesamer, P., Supalakorn, N., Koehler, K., Chailapakul, O., Henry, C. S., Volckens, J., 2013. Microfluidic paper-based analytical device for aerosol oxidative activity. Environ. Sci. Technol. 47 (2), 932–940.
Verma, V., Fang, T., Guo, H., King, L., Bates, J., Peltier, R., Edgerton, E., Russell, A., Weber, R., 2014. Reactive oxygen species associated with water-soluble pm 2.5 in the southeastern United States: spatiotemporal trends and source apportionment. Atmos. Chem. Phys. 14 (23), 12915–12930.
Vidrio, E., Phuah, C.H., Dillner, A.M., Anastasio, C., 2009. Generation of hydroxyl radicals from ambient fine particles in a surrogate lung fluid solution. Environ. Sci. Technol. 43 (3), 922–927.
Visentin, M., Pagnoni, A., Sarti, E., Pietrogrande, M.C., 2016. Urban pm2.5 oxidative potential: importance of chemical species and comparison of two spectrophotometric cell-free assays. Environ. Pollut. 219, 72–79.
Xiong, Q., Yu, H., Wang, R., Wei, J., Verma, V., 2017. Rethinking dithiothreitol-based particulate matter oxidative potential: measuring dithiothreitol consumption versus reactive oxygen species generation. Environ. Sci. Technol. 51 (11), 6507–6514.
Yamada, J., Matsuda, H., 1973. Limiting diffusion currents in hydrodynamic voltammetry: iii. Wall jet electrodes. J. Electroanal. Chem. Interfacial Electrochem. 44 (2), 189–198.